PROCEEDINGS of ISMA 2019
International Symposium on Music Acoustics
13 - 17 September 2019 in Detmold, Germany

Metamaterials in Musical Instruments *

Bader, R., Fischer, J., Münster, M. & Kontopidis, P.(1)

(1)Institute of Systematic Musicology, University of Hamburg, Germany, R_Bader@t-online.de

Abstract

Acoustic metamaterials are complex geometries leading to acoustic behavior not found in natural material, like negative stiffness or refraction, cloaking or spectral bandgaps. Indeed musical instruments are complex structures and some may already qualify as metamaterials. Still altering the instrument geometries and adding metamaterial behavior can increase the instruments sound variability and articulatory possibilities or lead to sounds not expected from mechanical instruments at all. The paper presents such examples. When modifying a frame drum by adding additional point masses forming a ring, the frame drum shows cloaking behavior when struck in the middle of the ring, where frequencies within a certain frequency band cannot leave the ring. This leads to a bandgap in the spectrum in the mid frequency range. Still when striking the drum outside the ring a normal drum sound is achieved. Therefore a drummer can produce sounds not known from drums before while with the same instrument can also play regular sounds. Other examples are modified guitar top plates with added point masses or waveguide structures.

Keywords: Sound, Music, Acoustics

1 INTRODUCTION

Metamaterials have not explicitly been used in musical instruments to this point. Still the complex geometry of musical instruments might lead to reconsider them as such. Although the fan bracing of guitars or the bracing of piano soundboards is built mainly for the purpose of stability, such regular substructures might lead to a behaviour meeting conditions of the concept of metamaterials. Indeed pitch glides of Chinese gongs [1], the brassiness of crash cymbals [2] or tam-tams [3], or the increased brightness of Balinese *gamelan gender* bronze plate [4] are caused by complex geometries.

Metamaterials in musical instruments can be used to change the instrument sound considerably. Changing existing instrument geometries can lead to added band gaps in their spectrum, and using several of such band gaps will lead to a designed sound. With percussion instruments musical articulation is realized by striking or knocking at different positions on e.g. drums or cymbals. By adding metamaterial structures to them the variability of such sounds can be increased considerably.

Membranes used in Rock or Jazz drum kits, as well as with *tablas* of Indian music or the *pat wain* or the Myanmar *hsain wain* orchestra often show additional masses attached to them. They are used for different purpose. Jazz drummers use tape and other material to damp especially the snare drum. Also tom-toms are taped to reduce the loudness as well as the length of their tone. Detuning of these drums play a minor role since these drums are tuned by tuning pegs at the drum head rim. *tabla* [4, 5] and *pat wain* [6] drums are tuned by adding a plate or a special tuning paste respectively. The aim is twofold, the drum is tuned with respect to its pitch and moreover the overtone spectrum of the drums is changed to arrive at a more harmonic overtone spectrum of the fundamentally inharmonic spectrum of these percussion instruments. The advantage of a more harmonic spectrum is to increase pitch perception of the drums to use them in melody performance.

Metamaterials have been used with membranes to achieve damping over a large bandwidth [7, 8], for a review see [9]. With massive rings attached concentric on the membrane one or only a few resonance frequencies exist up to 1 kHz, which leads to strong damping of the membrane within this range with large peaks at the resonance frequencies. Such applications differ from the concept proposed in this paper in its aims. There a strong overall damping is aimed for, where with musical applications only a partial damping is needed to maintain an audible sound. Also with such heavy masses the membrane between the mass and the membrane boundary, as well as the membrane between two rings can mainly be considered as a spring. As with concentric

*https://rolfbader.de/metamaterial-drum

rings the distances between the rings outer boundary and the membrane boundary is a constant for all angles, only one spring length and strength is present. So these applications differ in principle from the construction and the aims of the dot masses attached asymmetrically on a membrane present in this study.

Circular or more complex shaped geometries might result in a cloaking behaviour, where a traveling incoming wave looks the same in both cases, with the structure and without the structure in its way. Therefore for an observer behind the structure this structure is invisible [10]. Such geometries can also act as cages, where waves in them cannot travel out and vice versa. This has been found in optics [11] and has been applied in acoustics like in [12, 13] next to others. This behaviour is frequency dependent and a way to built a musical metamaterial, enhancing the articulatory ability of a musical instrument.

In this paper an example of applying metamaterial behaviour to musical instruments is demonstrated using a frame drum. It results bring on highly interesting new sounds and increased articulatory ability for players. After introducing the constructed instruments, the paper discusses the measurement techniques applied, microphone array and laser interferometry. Increased articulatory possibilities of the new instrument are discussed together with further design possibilities.

2 Methods

2.1 Frame Drum

A frame drum with a BoPET (biaxially-oriented polyethylene terephthalate) also called mylar drum membrane and a diameter of 40 cm was used. At the drumhead a ring-shaped area (m) with a diameter of 10 cm is separated using a set of 2×10 Neodymium magnets sticking at the front and the back of the membrane. The magnets are circular with a diameter of 5 mm and a height of 5 mm (see Fig. 4).

The magnet were chosen as they add a heavy mass to the membrane at distinctive points. When two magnets are attached to each other from the top and bottom side of the membrane the vibrations on the membrane are never strong enough to make the magnets move or fall off, no matter how hard the drum is struck. Additionally magnets are not damaging the membrane during attachment or when removing. They are also quite heavy with respect to their size. Yet a fourth advantage is that they can easily be moved by hand forming new structures. So musicians would be able to handle them easily. Still there is a lower distance limit between the magnets, as they will align magnetically. After experimenting with different adhesive fastening techniques, magnets were found to outperform other methods.

The area separated by the magnets is assumed to act as cloaking, separating vibrations inside and outside this area. Therefore it is expected that waves originating outside the ring will not enter and vice versa. In this case the frequencies and modes of one of the membrane areas are cloaked and do not contribute to the radiated sound. We therefore expect a band gap to appear in some cases where certain frequencies regions are not present. The cloaking of a frequency band, the band gap is then caused by a cloaking of regions on the membrane.

2.2 3D printed plates

Five square plates of dimension $40 \times 40cm$ were printed using a BigRep Studio-3D printer loaded with PLA-filament, a polylactic acid material printed at 205°C . The density of the raw material is $1.24g/cm^3$, the tensile strength (ISO 527) is $60MPa$, the impact strength (ISO 179) is $7.5KJ/m^2$, flexural modulus (ISO 178) of $3800MPa$. All the plates have a continuous thickness of 2mm with additional geometries printed on them. The five versions are described as followed:

1. Plain square plate, $40 \times 40cm$
2. Plate with two cups attached, open side oriented to -x-direction, with diameters of 5.5cm, 5.25cm depth, 3mm wall thickness, positioned at x=11-16.25cm, y=25cm and x=21-26.25cm, y=15cm respectively, relatively to the $40 \times 40cm$ dimension of the plate.

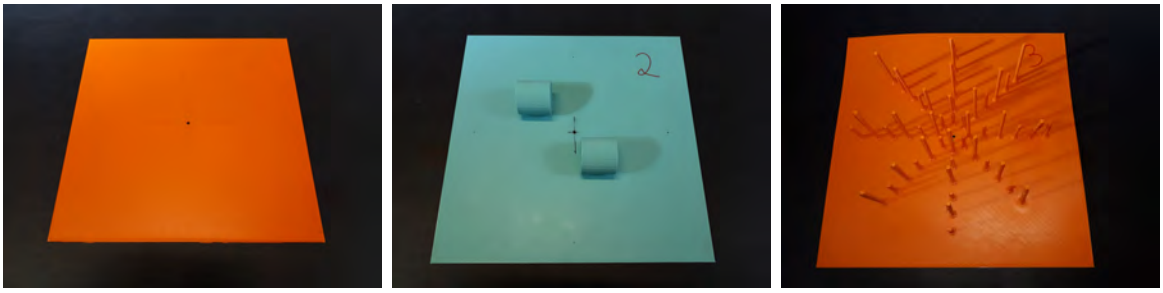

Figure 1. Square plates 1,2 and 3, from left to right.

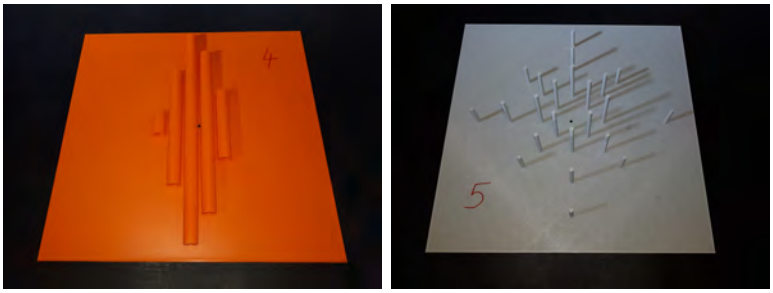

Figure 2. Square plates 4 and 5, from left to right.

3. Plate with 48 small rods arranged in z-direction, equally in line on medians and diagonals with a distance of 3cm, starting in the middle. There are 24 rods à $10cm$ and 24 rods à $5cm$, each have a diameter of 5mm.

4. Plate with five tubes lengthways an imaginary y-axis. The tubes are of different lengths: $3cm, 20cm, 36cm, 28cm$ and $12cm$ have a diameter of $2cm$ and $3mm$ thick walls. The longest tube is placed in the middle of the plate at $x = 20cm$, $y = 2$ to $38cm$. All the rest is arranged centered with a distance of 3cm to the adjacent tube.

5. Plate with twenty rods: 8 à $4cm$, 7 à $6cm$, 8 à $8cm$ each with a diameter of $5mm$. They are equally in line on medians and diagonals with a distance of $3cm$, starting in the middle of the plate.

The idea is to build geometries with spectral band gaps or enhanced spectral regions. The tubes and bars attached to the plain plate are assumed to resonate with discrete frequencies. Such vibrations can either take energy out of the plate or increase the radiation of these frequencies.

The bars are expected to take energy out, as their vibration is mainly in-plain, where the radiating area is only the top end area of the bars. This area is so small that no considerable radiation is expected. As the vibrations are damped in the bars due to internal damping, band-gaps in the radiation spectrum of the whole plate are expected at the discrete bar frequencies.

The tubes are expected to also take over energy from the plate, where the air inside the tube are driven by the plate. These frequencies are expected to radiate strongly. Theoretically, tubes with open ends have no radiation, except for the radiation caused by the end-correction of the tube. Here tubes with larger diameter have considerable larger radiation. Therefore two kinds of tube diameters were realized. The radiation due to the end-correction is also frequency-dependent, where lower frequencies radiate considerably louder than higher

ones. Therefore considerable radiation is expected for the lowest few modes. Therefore different tube length were used to address different fundamental frequencies. The radiation is also strongly directional-dependent, as the tubes were only added to one side of the plate.

2.3 Laser interferometry

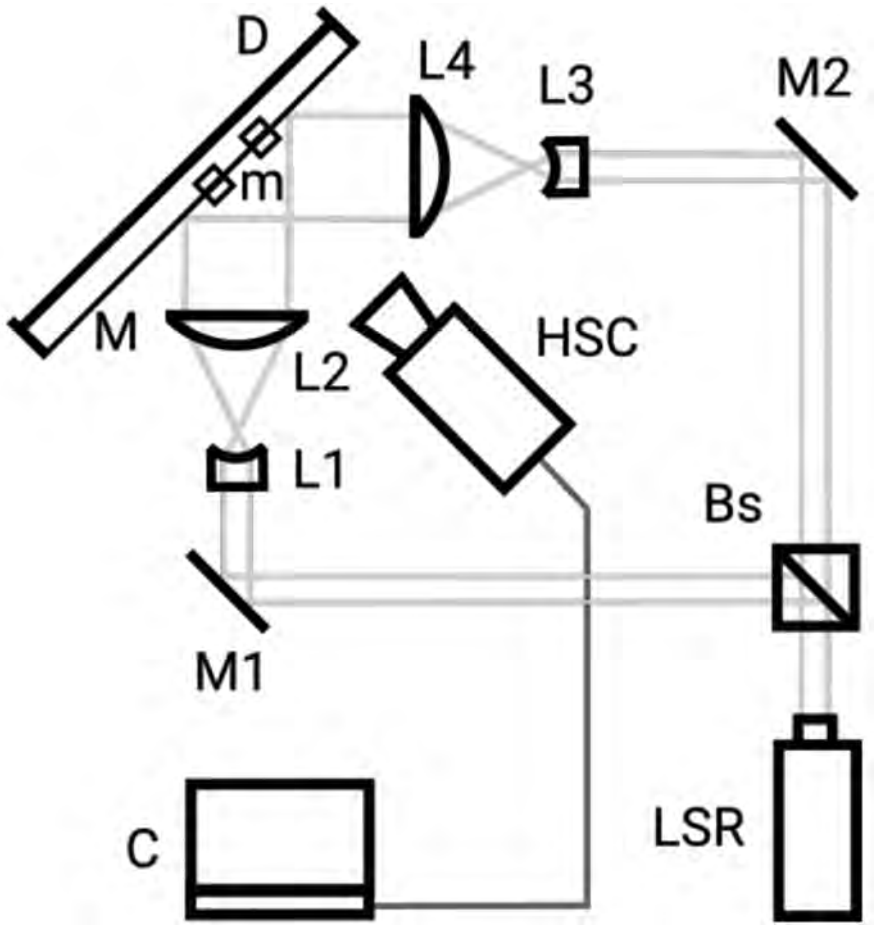

Figure 3. The experimental set-up. (LSR) laser, (Bs) Beam splitter, (M1, M2) planar mirrors, (L1, L3) semi-concave lenses ($f_{L1,L3} = -16\,mm, d_{L1,L3} = 10\,mm$), (L2, L3) semi-convex lenses ($f_{L2,L4} = 300\,mm, d_{L1,L3} = 100\,mm$), (M) drumhead of the frame drum (D), (m) circle-shaped part of the drumhead, separated utilizing a set of 2×10 Neodynium magnets. (HSC) high-speed camera, (C) analysis using a PC. The beam pathes are marked by green lines.

The experimental laser set-up is depicted in Fig. 3. A Verdi Single FAP (fiber array package) diode-pumped solid state frequency doubled Neodynium Vanadate ($(\mathrm{Nd}:\mathrm{YPO}_4)$ laser (LSR) source radiates a beam of wavelength $532\,nm$ and beam diameter of $d_{LSR} = 2.25 \pm 10\%\,mm$. The beam is splitted by a beam splitter (Bs). The splitted beams are directed to planar mirrors (M1) and (M2). Subsequently the beams are expanded via an optical lens system, consisting of a semi-concave lens with focal distance of $f_{L1,L3} = -16\,mm$ and a diameter of $d_{L1,L3} = 10\,mm$ and a semi-convex lens with focal distance of $f_{L2,L4} = 300\,mm$ and a diameter $d_{L2,L4} = 100\,mm$. The drumhead was manually excited by an impulse hammer. The excitation has been applied outside as well as

inside the separated area of the drumhead. The splitted and widened beams are directed to the drumhead (M) of a frame drum (D). The impulse response leads to a characteristic interference pattern at the drumhead. The pattern is recorded using a high-speed camera (HSC) with a frame rate solution of 10000 fps. The received data are analyzed utilizing Mathematica on a PC by subtracting adjacent recorded frames [14].

Additionally, the drum head was excited by an actuator, a Brüel & Kjaer Vibration Exciter 4809, again in the middle of the ring and outside with a low frequency of 65 Hz and a high frequency of 918 Hz, two eigenfrequencies of the drum head with magnets on.

2.4 Microphone Array

The sound pressure field of the frame drum was recorded with a microphone array in the near-field, 3 cm in front of the membrane (see Fig. 4). The grid constants of the array are 5cm in x-direction and 4cm in y-direction. The microphone array records sound fields with up to 128 microphones with a sampling frequency of 48kHz and a sample depth of 24 bit simultaneously.

The recorded sound fields are back-propagated to the surface of the membrane using the Minimum Energy Method (MEM) [15], a multipole-method assuming as many radiation sources as microphones. It has successfully been used to measure the vibrations of musical instruments [16, 17] (for a review on microphone arrays and back-propagation methods see [18].

For the recordings with the microphone array the drum was struck at three positions only, recorded with a single microphone placed 50cm in front of the membrane opposite, pointing to the drum center in an unechoic enviroment. Each recording resulted in 120 sound files at the microphone positions. From these the frequency spectra were calculated and all peaks up to 1 kHz were determined. For each of these frequencies the recorded sound field was back-propagated to the surface of the drum.

3 Results

3.1 Drum modes and traveling waves

The drum was struck at three different positions as it is expected that the ring acts as a cloaking effect to the sound and therefore striking within the ring should keep most of the vibrations within this ring, while striking outside the ring would lead to a strongly reduced energy in the ring. In Fig. 5 and Fig. 6 the results of the microphone array recordings and back-propagations are shown considering this point.

The results in Fig. 5 are calculated by first detecting the maximum absolute amplitude of each mode. The local positions of these maxima are accumulated on the membrane for all strikes. Then all points on the membrane showing more than 20% of accumulated maximum points are displayed.

At the top of Fig. 5 the case of striking in the ring is shown. Clearly most maximum points are within the ring. When striking at the ring rim, shown in the middle graph, the distribution of maximum amplitudes is more widespread over the membrane. Finally with the case of striking outside the ring, shown as the bottom plot in the figure, no considerable maxima are within the ring.

To differentiate this finding with respect to frequency, the amount of absolute amplitude within the ring is shown in Fig. 6 as a fraction of the whole absolute amplitude on the drum. The three curves show the three cases of striking in the ring, at the ring rim and outside the ring. Again striking in the ring leads to a strong increase of amplitudes within the ring, compared to the cases of striking at the ring rim and outside the ring. Still this increase only appears above about 400 Hz. As the fundamental frequency of the drum is 34 Hz we can conclude that the low frequencies are not much effected by the ring, while the higher ones clearly are.

Still the relative high fraction of amplitudes in the ring at very low frequencies are again remarkable. The lowest peak detected at 7 Hz is not audible and most likely refers to the motion of the drum as a whole, so including the wooden frame. This motion is unavoidable as frame drums only sound when the wooden frame is free. Fixing it strongly, which would avoid this low vibration would lead to a very much damped sound and can therefore not be implemented in an experimental setup.

Figure 4. Modified frame drum positioned in frot of the microphone array.

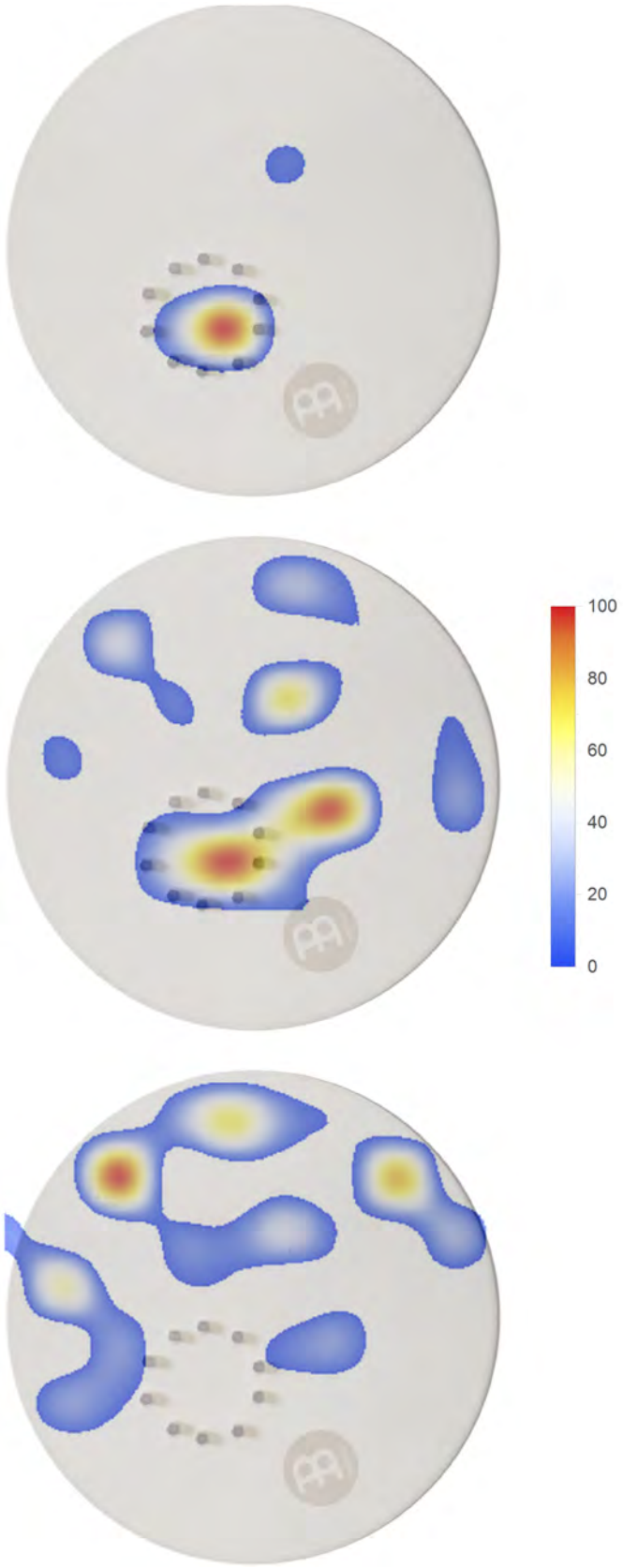

Figure 5. Density distribution of maximum amplitude values of modes on the drum up to 1 kHz for three hammer strike positions, showing densities above 20%. Top: strike in the circle, Middle: strike at circle rim, Bottom: strike outside the circle at the opposite side of the circle. While most maximum values for the strike in the circle are in the circle, very few are within the circle when the drum is struck outside the circle. A medium case is found when striking at the circle rim.

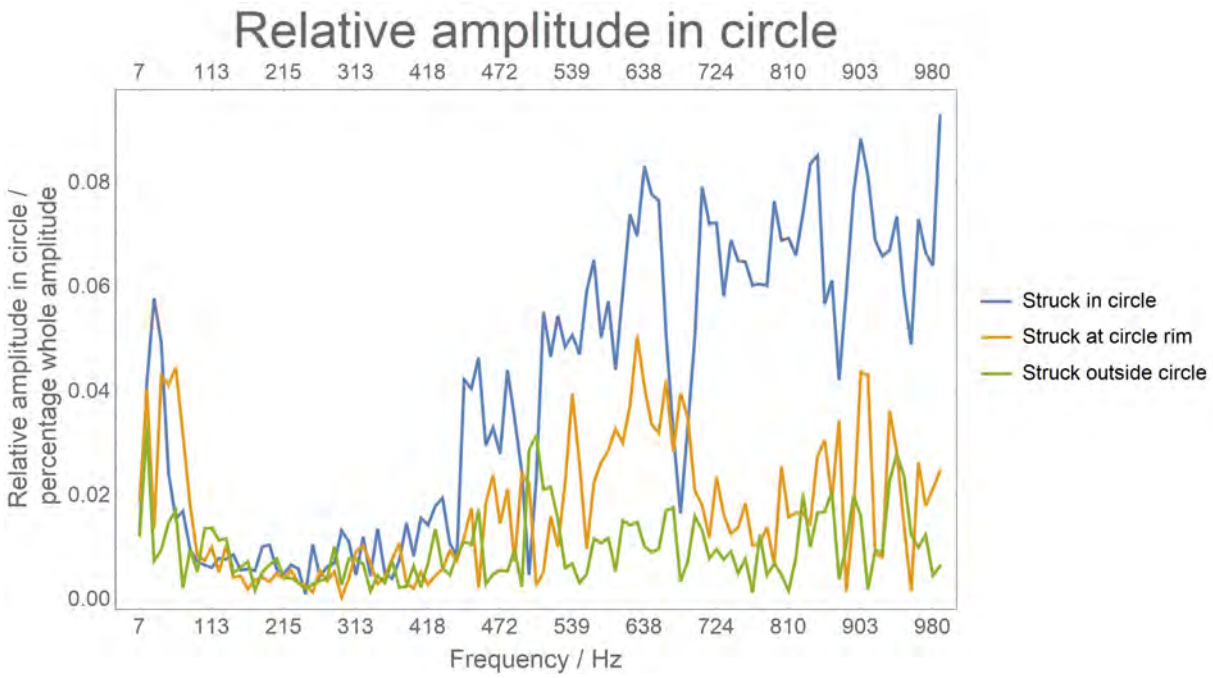

Figure 6. Frequency-dependent absolute amplitude within the circle compared to total absolute amplitude on the whole drum for three strike cases a) in the circle (blue), b) at the circle rim (orange), and c) outside the circle (green). While for frequencies below around 400 Hz the amplitude strength of the three cases are about the same, above about 400 Hz the amplitude strength within the circle strongly depends on the strike position. Strikes in the circle have stronger amplitudes there than strike at the rim with strike outside the circle showing least amplitudes in the circle.

Still the very low frequencies at 34 Hz, the 'monopole' vibration and around 65 Hz, the 'dipole' vibration again show much more relative amplitude within the ring in the cases of striking in the ring and striking at its rim, compared to the case of striking outside the ring.

The reason for this behaviour can be found when examining the modes more closely. The very low modes need to make the ring region move, too, as the anti-node regions are large, with 34 Hz it basically covers the whole membrane, with the 65 Hz 'dipole' case the membrane is split into two regions about half the membrane each. Of course due to the ring no monopole and dipole modes exist as in the case of a isotropic membrane.

The higher modes above the dipole, quadrupole, octopole and many other more complex modes with an integer number of axial and circular nodal lines, these modes can deform in such a way to avoid the motion of the ring region nearly completely. This holds for all three strike cases. It seems that even when striking in the ring, the ring is not able to maintain a vibration of these frequencies. The small leakage of vibrations leaving the ring is then taken over by the rest of the membrane leading to very similar motion compared to the case when striking outside the membrane.

To confirm these findings in Fig. 7 laser interferometry measurements for the case of striking in the ring are shown. The strike's transient is displayed as six snapshots at 0 ms, 0.2 ms, 0.6 ms, 1 ms, 3 ms, and 6 ms. Each black/while line indicate an amplitude increase of one wavelength of the used laser light. Therefore many rings do not indicate an amplitude ripple but a steep slope of the amplitude.

Starting at 0 ms, the strike leads to a circular wavefront leaving the strike point, shown at 0.2 ms. At about 0.6 ms this circular wavefront meets the ring rim. Here is is scattered and at the open rim positions new wavefronts

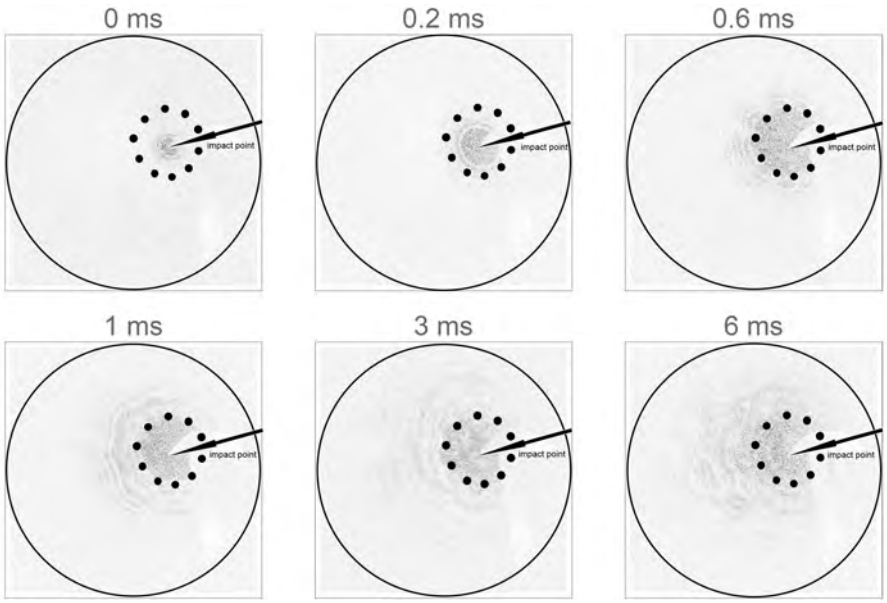

Figure 7. Laser interferometry time-dependent measurement of the initial transient of a hammer strike on a drum with a separated cirular area for several time steps. At 0 ms a circular wave leaves the strike point which meets the circle boundary at about 0.2 ms. The boundary elements lead to a split of the circle and the appearance of Huygens wave fronts outside the circle beyond 0.6 ms. At 3 ms the reflected waves on the membrane lead to complex vibrations.

start, as expected. At 1 ms these wavefronts form another wavefront outside the ring, slightly ripped as this wavefront is formed from a finite number of elementary waves according to the Huygens principle. Two cases at 1 ms and 3 ms show the wavefront outside the ring becoming more and more complex as the wavefront is then already reflected at the drum boundaries and leads to a complex waveform.

Still it can be seen at 1 ms that the ring still has a strong amplitude, much stronger than that leaving the ring. This picture continues at 3 ms and 6 ms supporting the findings fr om above. Again most vibrations are overall kept out of the ring when striking.

The same transient time development when striking outside the ring is shown in Fig. 8. Again at 0 ms a circular wave leaves the impact point which arrives at the ring at about 0.6 ms. At 1 ms it can be seen that the strong amplitude is still present outside the ring while only a small fraction enters the ring. This continues at 3 ms. At 6 ms there is some energy left in the ring likewise, which is expected from the above findings, namely that for very low frequencies at 34 Hz and 65 Hz, the ring region is also moving with some amplitude. Still again overall most vibrations keep out of the ring when striking.

To differentiate the low / high frequency difference further, the drum is driven by a shaker in and outside the ring at two frequencies, 65 Hz and 918 Hz. In Fig. 9 snapshots of the vibrations are shown at maximum amplitudes of the sinusoidal vibrations. On the top row the 65 Hz cases are shown, at the left the case when driving in the ring, at the right when driving at outside the ring. Clearly in both cases broad vibrations can be seen, indicating a distorted dipole motion. Although when driving inside the ring the amplitude is stronger inside than outside, some amplitude is still outside. When driving outside, the amplitude is about equally distributed. This is in accordance with the findings of the microphone array, especially with that of Fig. 6. There in all striking cases energy in the ring was present, still when striking in the ring the energy was even stronger.

The two lower plots in Fig. 9 show the laser interferometry measurements for sinusoidal excitation at 918Hz

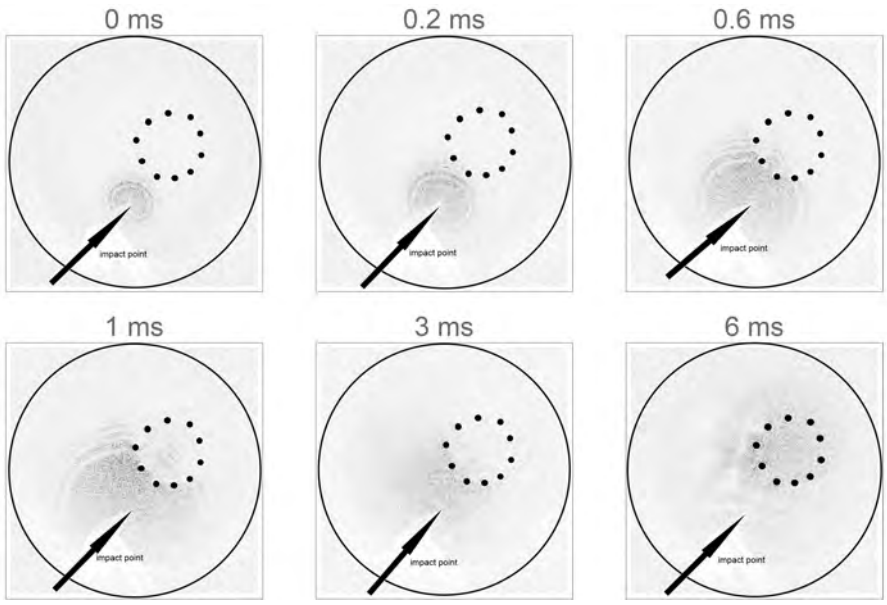

Figure 8. Laser interferometry measurement of a hammer strike on a membrane with a separated circle area, striking outside the circle. A circular wavefront leaves the strike position and reaches the circle boundary at 0.2 ms. The boundary leads to a formation of a Huygens wavefront inside the circle from about 0.6 ms. From 1 ms on the vibrations inside the circle are much less than those outside. Still after about 6 ms there is motion inside the circle, still at small wave vectors and therefore at low frequencies only.

inside the ring on the left and outside on the right. Clearly when driving inside the ring nearly all amplitude are within the ring, while when driving outside nearly all amplitudes are outside the ring, while the ring boundary cloaks the inner ring area.

Clearly the ring is cloaking vibrations in both directions, from within the ring to its outside and vice versa for frequencies above about 400 Hz. For frequencies below 400 Hz it is cloaking in a way that vibrations from outside do not enter the ring. Still when driving the ring some vibrations escape the ring and form modes outside. But also in this case the ring is not taking part in the vibrations considerably. For very low frequencies the cloaking becomes uneffective which is caused by large anti-nodal areas on the membrane.

3.2 Example sounds

The drum sounds considerably different when struck inside or outside the ring. Within the ring a sound is produced not known from regular drums, while when struck outside a normal drum sound appears. To display this aural finding the drum was struck at three positions only recording the sound with a single microphone 50 cm in front of the membrane opposite to the drum center in an unechoic chamber. With a wooden hammer the drum was struck right at the center of the ring, at the ring boundary between the magnets at a place most close to the membrane center, and outside the ring opposite to it, still with the same distance to the membrane boundary as the ring center, which is 13.5 cm.

Additionally, to test the influence of different ring diameters, next to the 10 cm diameter used for the measurements above, two additional rings were built, one with 8 cm and one with 12 cm in diameter. All had the same center point of the ring as the 10 cm ring, i.e. 13.5 cm in radial distance to the membrane boundary.

The here produced sounds are exemplary. A vast variaty of sounds can be produced utilizing hammers of different geometries, elasticities and hardnesses. The test strikes were performed with musical accuracy providing

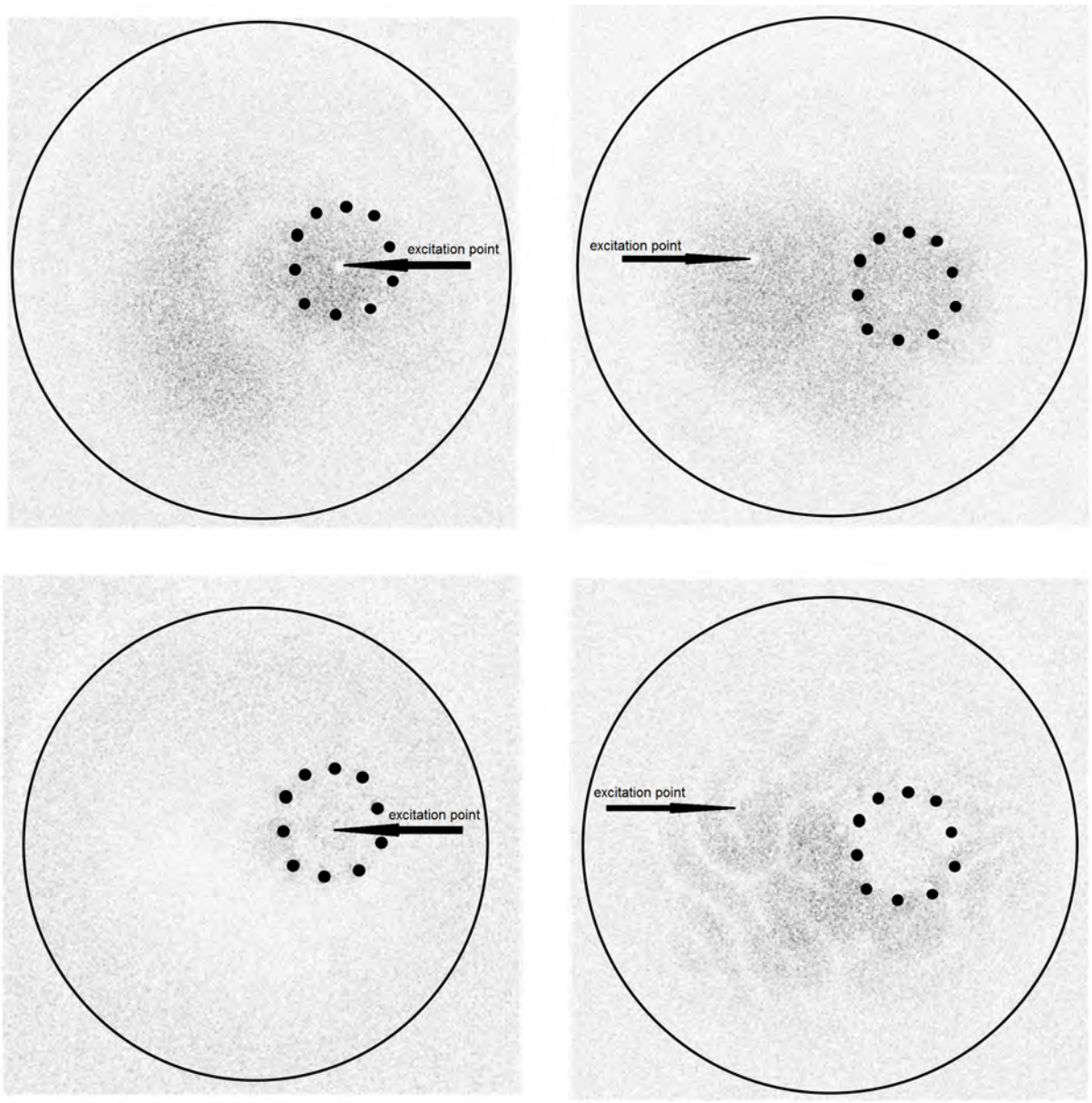

Figure 9. Snapshots of forced oscillations at 65 Hz (top row) and 918 Hz (bottom row) inside (left column) and outside (right column) the circle. At the low frequency at 65 Hz the vibrations are strong both, inside and outside the circle. At the high frequency of 918 Hz the driving of the membrane inside the circle only leads to a vibration inside, while driving the membrane outside the circle the movement is only outside the circle and very low amplitudes are present in the circle. Therefore the circle at this frequency of 918 Hz acts as a cloaking of waves in both directions. Comparing with Fig. 6 allows the conclusion that above about 400 Hz the circle acts as a cloaking element.

best possible uniformity in speed, strength and impact position.As the resulting sounds were so considerably different and this difference maintained when using different striking strength, the overall sound difference between the striking points is clearly documented by this method.

Fig. 10 shows the nine strikes, three diameters combined with the three striking positions. Each spectrum was calculated with a Fourier transform of the first 50 ms of the sound. As the drum is a percussion instrument the sound character is mainly heard during this initial sound phase. So the results presented here only refer to the initial transient.

In the top plot the spectra for the strikes inside the drum are displayed. They show a band gap starting from about $\sim$ 300 Hz - $\sim$ 700 Hz. The low frequencies are still strong, which also holds for the higher ones.

Contrary, the strikes outside the membrane displayed at the bottom of Fig. 8 show no such band gap but rather a regular spectrum exponentially decaying with frequency. The strike at the ring boundary displayed in the middle plot shows a mixture of both plots, again with an unusual flat spectrum, not considerably decaying towards the higher frequencies.

Both, the spectra of the strike inside the ring and that at its boundary cannot be produced by a regular drum. But as the drum can still be played outside the ring with regular spectral shape, it can still produce normal drum sounds. So adding the ring increases the articulatory possibilities of the drum considerably.

3.3 Theoretical Considerations

From this parametric study we can make estimations on the frequency on- and offset of the band gap.

3.3.1 Band gap upper cut-off frequency

From the lowest frequency of the membrane without the ring of $f_0 = 78$ Hz one finds a wave speed $c = f_0/J^0/(2\pi r) = 44.8$ m/s, where $J^0 = 2.405$ is the first zero crossing of the Bessel function as radial solution of the circular membrane wave equation with boundary conditions of zero displacement and drum radius $r = .2$ m. The wavelength λ fitting between two adjacent magnets of the ring is

$$\lambda_i = 2\pi r_i/m_n - m_d \tag{1}$$

with index i=1,2,3 for the three rings with radii $r_1 = .04$ m, $r_2 = .05$ m and $r_3 = .06$ m. Here $m_d = 0.005$ m is the magnet diameter subtracted from a $1/m_n$ of the ring circumference, with $m_n = 10$ the amount of magnets. The frequencies of these wavelength then are $f_i = c/\lambda_i$, and therefore $f_1 = 2027$ Hz, $f_2 = 1545$ Hz, and $f_3 = 1247$ Hz.

These frequencies are about twice the upper cut-off frequency of the band gap at about 700 Hz - 800 Hz. Therefore the cloaking behaviour disappears when the gap between the magnets is half the wavelength of the respective frequency. In Fig. 5 (top plot) the tendency of smaller ring diameters to have a larger band gap can clearly be seen. The 8 cm ring has a much larger band gap up to about 800 Hz, the 10 cm ring has a spectral peak at about 550 Hz and the 12 cm ring has also a peak at about 550 Hz but is much less damped before this frequency range. Indeed the band gap has a small amplitude slope in and out and is not a straight cut at the cutoff-frequencies (has a low Q when taken as a filter). This is expected as the calculated frequencies assume perfectly rigid magnets with infinite mass which is not the case. Still clearly the higher cut-off frequency is determined by the ring size.

As found with the microphone array and the laser interferometry data, the magnets prevent the waves within the band gap to leave or to enter the ring. The corresponding wavelengths are much longer than the distances between the magnets. Therefore the magnet geometry is sub-wavelength and therefore the effect is not a simple scattering but a cloaking of waves. When struck in the ring these band gap frequencies stay within the ring and therefore have a much smaller radiation area compared to waves traveling over the whole membrane, the lower and higher frequencies. This leads to lowered amplitudes of the band gap frequencies in the radiated sound.

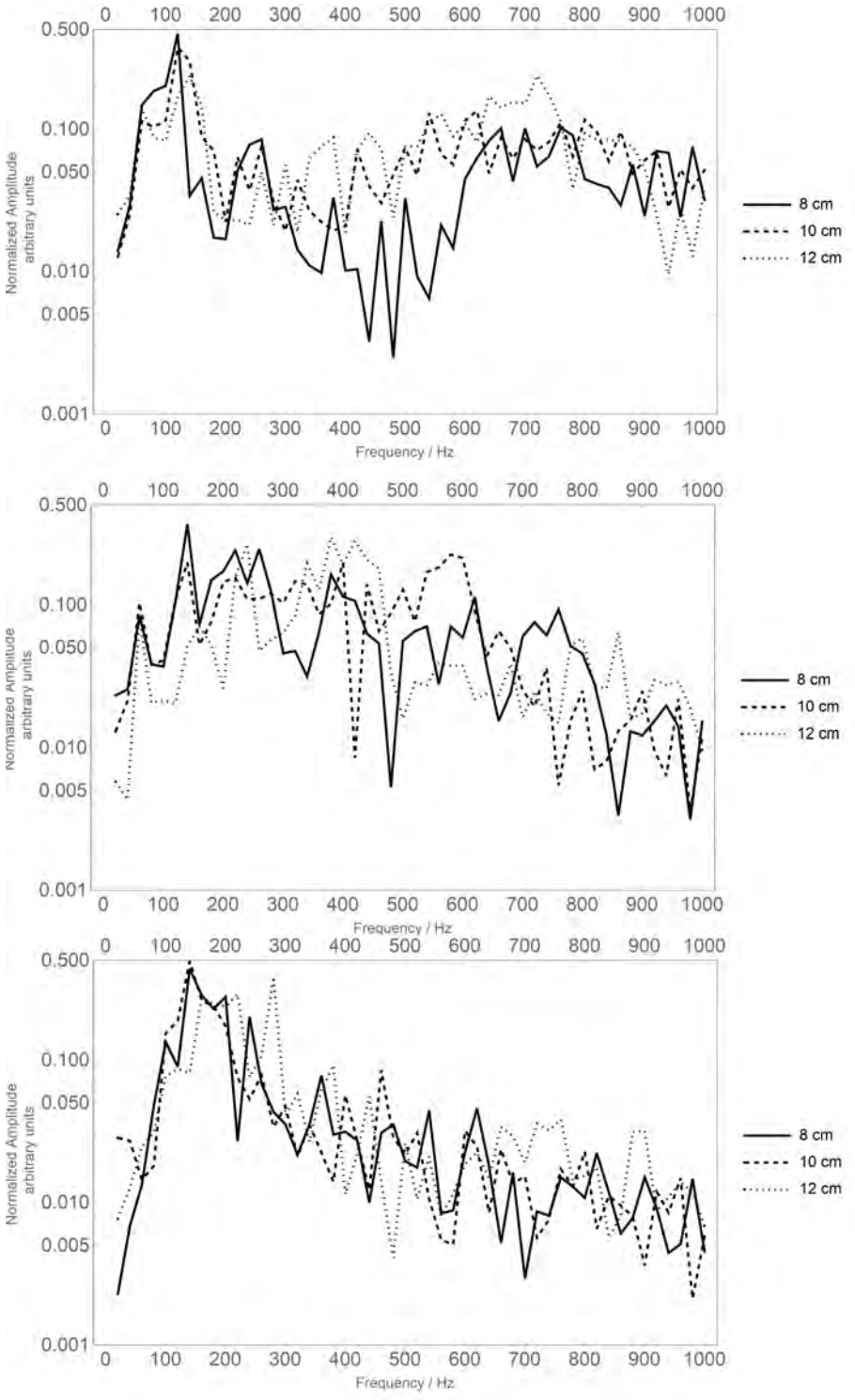

Figure 10. Spectra of example strikes on the modified membrane for three ring diameters, 8 cm, 10 cm, and 12 cm, as Fourier analysis of the first 50 ms of sound, top: strike position at the ring center, middle: strike position at the ring boundary, bottom: strike position outside the ring. The strikes inside the ring show a band gap between 300/400 - 700/800 Hz, the strikes outside the ring show regular decaying overtone strectra, the strike at the ring boundary are in the middle between inside and outside strikes.

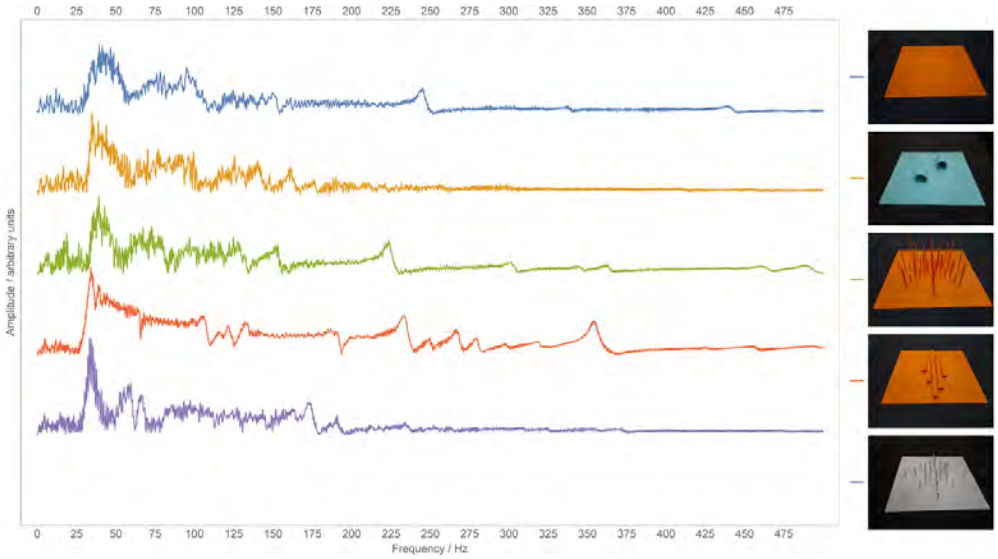

Figure 11. Spectra of five metamaterial plates of 40×40 cm, the elevation is arbitrary to have a better display, the amplitude axis is linear. From top to bottom: a) plain plate, b) plate with two large tubes, c) plate with bars, d) plate with five tubes, e) plate with bars (see text for details). The spectra of the modified plates show frequency regions of in- or decreased energy, as expected.

3.3.2 Band gap lower cut-off frequency

Estimating the frequencies within the rings by taking the magnets as boundary conditions of zero displacement we find $f_1^0 = 390$ Hz, $f_2^0 = 312$ Hz, and $f_3^0 = 260$ Hz. This is not perfectly true of course and the movement present at the magnets might be taken as an enlargement of the radii to come closer to the real values. Still the values are around the frequency range where the band gap start. This confirms the finding of the microphone array data and the laser data. Frequencies below the eigenresonance of the ring appear over the whole membrane and are therefore not damped in the spectrum as those above the fundamental frequencies of the ring.

The ring diameter does not change this overall behaviour, still the 8 cm diameter has the strongest band gap, while the 10 cm and 12 cm rings perform similar (Fig. 8 top). This also holds for the strike at the ring boundary. Aurally, indeed the ring with the smallest diameter of 8 cm showed this band gap effect most clearly.

3.4 Metamaterial plates

The plates were investigated using the actuator driving recording the acceleration with a single piezo Fourier transforming the time series, as well as using the recording of a 128 microphone array and analyzing the decay with a T60.

3.4.1 Comparison using the actuator

Fig. 11 shows the spectra of the five plates using the actuator. All have a strong frequency range below 50 Hz, still with different sharpness. The plate 2 (second from top) with two large tubes have a smoothed spectra compared to plate 1. Plate 4 (second from bottom) with five tubes on the other side has a much more complicated spectrum. Plate 3 (third from top) with many bars is more lively in its spectrum compared to plate 5 (bottom) with only a few bars. Still this last plate has the sharpest peak at the lowest frequencies.

Fig. 12 shows comparisons of the spectra. The reference spectrum of plate 1 (top) has been kept like in Fig. 11. From all other spectra that of plate 1 was subtracted. The baselines for each spectrum is platted as a

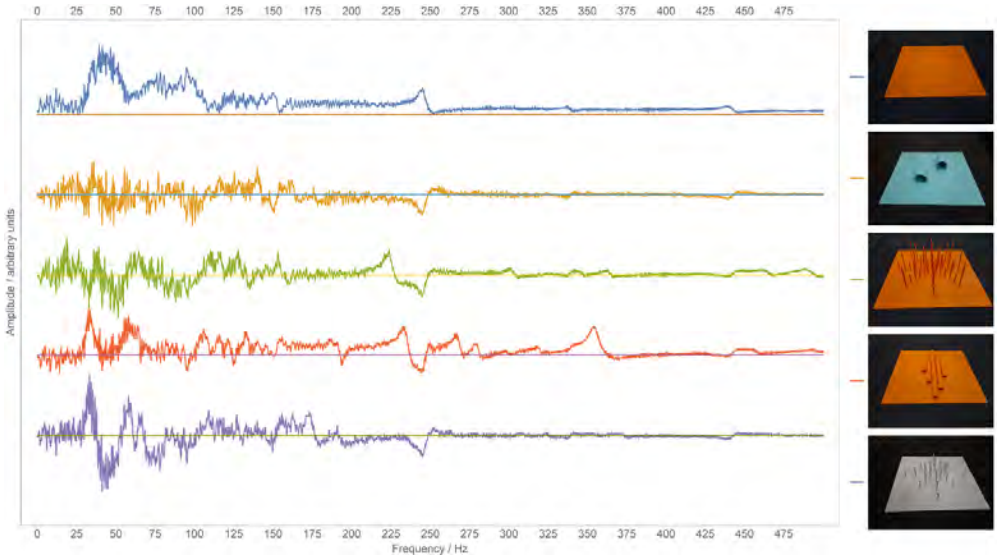

Figure 12. Comparison of spectra from Fig. 11. Plate 1 on the top is left like in the precious figure, all other are subtractions of spectrum of plate 1 from the respective spectra of plate 2 - 5. The lines are the zero line. Plate 4 (second from bottom) shows considerably more energy, while the other plates are more or less equal. Integrating the spectrum of plate 1 and weighting all other difference spectra with it plate 4 has 0.481% more energy than plate 1 within this frequency range. Contrary, plate 3 has only a 0.0556% increase, and plate 2 with -0.018% and plate 5 with -0.042% show a slight decrease.

horizontal line in the figure.

Plate 4 (second from bottom) shows considerably more energy, while the other plates are more or less equal. Integrating the spectrum of plate 1 and weighting all other difference spectra with it plate 4 has 0.481% more energy than plate 1 within this frequency range. Contrary, plate 3 has only a 0.0556% increase, and plate 2 with -0.018% and plate 5 with -0.042% show a slight decrease.

This is pointing to the tubes to be very effective. Indeed plate 4 shows the most lively spectrum and is considerably different from that of plate 1. This is most likely caused by the resonances in the air columns of the tubes.

Still the other spectra are different too. Plate 5 (bottom) shows strong deviations especially in the low frequency range around 50 Hz in both directions. Plate 3 (third from top) is much smoother , still considerable also in the low frequency range.

All plates sound very different aurally, when knocking on them. So all deviations are audible.

It is interesting to see that the impact appears strongly in the low frequency range, although the added geometries are all small, where impact in higher frequency regions is expected. Still the influence of many small geometries on frequencies in the sub-wavelength range of these geometries is a major aspect of metamaterials. Still other behaviour might play a role too, like the stiffening of the plate by the tubes.

4 Conclusions

The cloaking of the ring is frequency-dependent because the ring is not in a free-field but on a membrane which again has boundaries leading to eigenmodes of the whole system. For high frequencies above 300/400 Hz the eigenmode shapes outside the ring are complex enough that the membrane acts very much like a free field and therefore the regular cloaking behaviour appears. For lower frequencies, here below 300/400 Hz, cloaking still

works in one direction that waves from outside do enter the ring not considerable, still when driving within the ring waves can leave to the outside area. For very low frequencies the cloaking then nearly vanishes. Above about 700/800 Hz the waves again travel freely over the ring boundary as the wavelength are smaller than the distances between the magnets.

The transient laser interferometry measurements also show that when striking the drum in the ring, at the very beginning of the sound some energy leaves the ring. These vibrations trigger the modes between about 100 Hz and 400 Hz outside the ring and those above the upper cut-off frequency of the band gap. This offers another musical option to decide which frequency range to drive when striking in or outside the ring.

It also appears that when striking at the rim of the ring a mixture of the two extremes, striking outside the ring or at the very center of it can be achieved. This holds for both, the frequency range up to about 400 Hz and that above this range.

Furthermore the cloaking of the ring leads to a different radiation behaviour of the drum compared to when struck outside the ring. When at higher frequencies only the ring area vibrates, it acts like a monopole and radiates sound from a clearly defined point. When striking outside the ring complex modes appear with a completely different radiation behaviour. Therefore depending on the driving point the same frequency might have two completely different radiation patterns. As a monopole radiation is perceived as a loudspeaker-like source, while a complex radiation pattern is perceived as a musical instrument played live a musician has a new kind of articulation with such a manipulated drum.

The drum shows a much higher amount of timbre variability compared to a regular drum. With regular drums the drummer can only vary the sound by striking at different positions, where striking in the middle leads to a sound dominated by low frequencies and striking more to the edge increases the amount of energy at higher frequencies making the sound more bright. Although when striking outside the ring with the presented manipulated drum these articulations are still possible, additionally the drummer is able to produce completely new sounds, when striking the membrane at different positions within the ring.

When striking at the very center, even very strongly, the sound has only energy in the low frequencies, with a band gap from 300/400 Hz - 700/800 Hz. Higher frequencies appear only in the initial transient as they decay naturally very fast. The amplitude attenuation in the band gap incrases with smaller ring diameters. This sound is not known from a regular drum struck in its middle as due to the transient behaviour of such a strike and the band gap discussed above at the very beginning of the tone higher partials are present more than with a regular drum struck at the drum center. Therefore such a sound is not possible to produce for drummers with regular drums.

The metamaterial plates show a considerably different frequency-dependent mobility. Especially plate 4 with the long tubes have amplitude peaks at small-band frequency ranges between 225-300 Hz. This plate is also resonating stronger than the reference plate 1 nearly all over the range up to 500 Hz. Therefore this plate construction is expected to be both, louder than the reference plate and enhancing special small-band frequency bands. These frequency bands need to be related to the resonance frequencies of the tubes, which is subject to further studies.

Plates 3 and 5 with the added bars show in- and decreased mobility, especially in the low frequency range around 30-50 Hz. Again this is a typical behaviour of metamaterials, where small scale geometries in the sub-wavelength size of lower frequencies effect these low frequencies. The plate with the shorter bars shows a stronger influence compared to the plate with the longer bars.

Plate 2 with the short tubes with large diameter smooth the spectrum from about 200 Hz on. Also in the low range it smoothes the spectrum compared to the reference spectrum of plate 1.

It appears that metamaterial plates are able to effect plate mobility, produce small-band gaps and peaks and effect very low frequency ranges around 20-40 Hz.

5 Acknowledgements

Many thanks to those helping with the measurements of the plates: Niko Plath, Paul Testa, Jakob Schenke, Carola Ohlsen, Pascal Brunet, Bela Wiener and Simon Mayrshofer.

References

[1] M. Jossic, O. Thomas, V. Denis, B. Chomette, A. Manmou-Mani, and D. Roze, D., "Effects of internal resonances in the pitch glide of Chinese gonsg," J. Acoust. Soc. Am. **114**, 431-442 (2018).

[2] C. Touzé, and A. Chaigne, "Lyapunov Exponents from Experimental Time Series: Application to Cymbal Vibrations," Acustica **86**, 557-567 (2000).

[3] Th. D. Rossing, *The Science of Percussion Instruments,* World Scientific, Singapore (2001).

[4] S. Tiwari and A. Gupta, "Effects of air loading on the acoustics of an Indian musical drum," J. Acoust. Soc. Am. **141** (4), 2611-2621 (2016).

[5] G. Sathej, and R. Adhikari, "The eigenspectra of Indian musical drums," J. Acoust. Soc. Am. **126** (2), 831-838 (2009).

[6] R. Bader, "Finite-Difference model of mode shape changes of the Myanmar pat wain drum ring using tuning paste," Proc. Mtgs. Acoust. **29**, 035004 (2016).

[7] Ch. J. Naify, Ch.M. Chang, G. McKnight, and S. Null, "Transmission loss of membrane-type acoustics metamaterials with coaxial ring masses," J. of Applied Physics **110**, 124903-1-8 (2011).

[8] H. Tian, X. Wang, and Y.-H. Zhou, "Theoretical model and analytical approach for a circular membrane–ring structure of locally resonant acoustic metamaterial," Applied Physics A. Materials Science & Processing, **114**, 985-990 (2014).

[9] T.-Y. Huang, Ch. Shen, and Y. Jing, "Membrane- and plate-type acoustic metamaterials," J. Acoust. Soc. Am. **139**, 3240-50 (2016).

[10] M.R. Haberman and A.N. Norris, "Acoustic Metamaterials," Acoustics Today **12** (3), 31-39, (2016).

[11] A. Mirzaei, A.E. Miroshnichenko, I.V. Shadrivov, and Y.S. Kivshar, "Optical Metacages," Physical Review Letters **115**, 215501-1-5 (2015).

[12] A. Colombi,Ph. Roux, S. Guenneau and M. Rupin, "Directional cloaking of flexural waves in a plate with a locally resonant metamaterial," J. Acoust. Soc. Am. **137** (4), 1783-89 (2015).

[13] M. Dubois, Ch. Shi, Y. Wang and X. Zhang, "A thin and conformal metasurface for illusion acoustics of rapidly changing profiles," Applied Physics Letters **110** 151902-1-5, (2017).

[14] Th. Moore, "Measurement Techniques," In: Bader R. (eds) *Springer Handbook of Systematic Musicology*, Springer, Berlin, Heidelberg, 81-103 (2018).

[15] R. Bader, "Reconstruction of radiating sound fields using minimum energy method," J. Acoust. Soc. Am. **127** (1), 300-308 (2010).

[16] R. Bader, "Characterizing Classical Guitars Using Top Plate Radiation Patterns Measured by a Microphone Array," Acta Acustica united with Acustica **97**, 830-839 (2011).

[17] R. Bader, "Radiation characteristics of multiple and single sound hole vihuelas and a classical guitar," J. Acoust. Soc. Am. **131** (1), 819-828 (2012).

[18] R. Bader, "Microphone Array," In: T. Rossing (ed.): *Springer Handbook of Acoustics*, 1179-1207 (2014).

[19] P.A. Deymier (ed.), *Acoustic Metamaterials and Phononic Crystals.* Springer Berlin Heidelberg (2013).

[20] D. Diderot, *Encyclopédie, Ou Dictionnaire Raisonné,* Vol. **66**: Suite Du Recueil De Planches. Cap.: Luthier, Planche I, Figure 8, (1779).

[21] R. Bader, "Additional modes in a Balinese gender plate due to its trapezoid shape," In: R. Bader, Ch. Neuhaus, and U. Morgenstern (eds.), *Concepts, Experiments, and Fieldwork: Studies in Systematic Musicology,* Peter Lang Verlag, Frankfurt a.M., 95-112 (2009).